Porous high-T_c superconducting cuprates: Advantages and applications

IOP Conf. Series: Journal of Physics: Conf. Series **1293** (2019) 012009 doi:10.1088/1742-6596/1293/1/012009

Porous high-T_c superconducting cuprates: Advantages and applications

M. R. Koblischka[1,2], A. Koblischka-Veneva[1,2], S. Pavan Kumar Naik[2], D. Gokhfeld[3], M. Murakami[2]

[1] Experimental Physics, Saarland University, P.O. Box 151150, 66041 Saarbrücken, Germany
[2] Superconducting Materials Laboratory, Department of Materials Science and Engineering, Shibaura Institute of Technology, Tokyo 135-8548, Japan
[3] Kirensky Institute of Physics, Federal Research Center KSC SB RAS, Krasnoyarsk, 660036, Russia

E-mail: m.koblischka@gmail.com; miko@shibaura-it.ac.jp

Abstract. Porous high-T_c superconducting cuprates are promising materials representing an alternative preparation route to enable the fabrication of large-scale, light-weight superconducting samples. There are several advantages of such samples including the much easier (and faster) oxygenation process, a simpler scalability to produce large samples, and of course, the reduced weight. Two different types of such samples were prepared in the literature: (i) Superconducting foams, prepared using polyurethane foams converted to green phase foams followed by an infiltration growth (IG) process. (ii) Superconducting nanowire networks prepared by spinning from sol-gel precursors. Such fabric-like nanowire networks are extremely light-weight, but show very interesting properties. We discuss the properties of such samples concerning both the physical parameters and the respective microstructures and give an overview about possible applications.

1. Introduction

Most research activities in the field of high-T_c superconductivity (HTSc) are focused to increase the critical current densities for various classical applications like energy transport and generation of high magnetic fields [1,2]. This forces to improve the crystallographic texture and to provide strong flux pinning. The corresponding materials are three types of HTSc samples: Tapes or wires, thin films and bulk samples. However, all of these sample types have certain drawbacks which hinder the development of some types of applications. One issue is, e.g., the scalability and shaping to obtain large superconducting samples of various shapes [3], the mechanical stability when generating large magnetic fields [4] and the problems arising when oxygenating bulk samples. In the latter case, the required time to oxygenate large, bulk samples requires weeks, and internal cracking may appear due to the phase transformation in the Y-Ba-Cu-O system ($YBa_2Cu_3O_{6...6.5} \rightarrow YBa_2Cu_3O_{6.6...7}$) [5]. As an answer to these problems, one can find in the literature several attempts to grow different types of high-T_c superconducting samples. In many current fields of research, porous metallic or ceramic samples play an increasingly important role as it becomes possible to produce light-weight samples with increased mechanical strength [6–9]. For superconducting porous samples, there are several adantages like (i) the easy and fast oxygenation process due to the open-porous structure, (ii) the scalability of the sample

size, (iii) the ideal cooling process and (iv) the reduced weight and the reduced amount of (expensive) superconducting (precursor) material. Therefore, some years ago, several different types of porous material were studied [10–15], but the further development of these materials was overrun by the progress of preparing coated conductors [16, 17]. However, even up to date, the aforementioned problems are not yet overcome, and certain applications are only possible with, or still require, the use of porous superconducting materials.

2. Experimental procedures

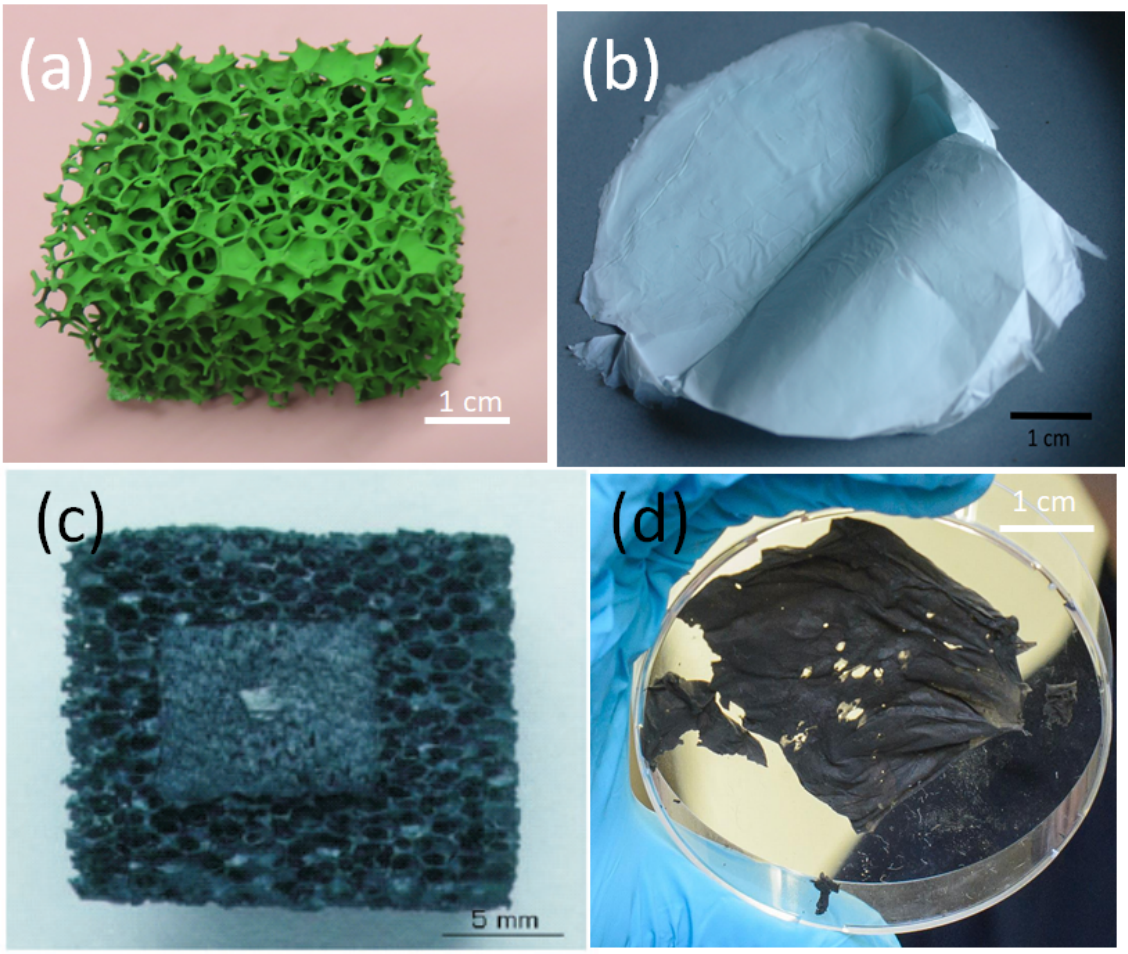

Figure 1. YBCO foam (a,c) and Bi-2212 nanowire network fabric (b,d). The images (a) and (b) give the preforms of both types of porous HTSc samples, and (c) and (d) the fully-reacted, final products. Note the seed crystal and the YBCO cloth on the foam surface in (c), and the size of the nanowire fabric samples in (b) and (d).

In the present contribution, we focus on two distinctly different porous HTSc materials: Bulk-like $YBa_2Cu_3O_y$ (YBCO) foams and $Bi_2Sr_2CaCu_2O_{8+\delta}$ (Bi-2212) nanowire network fabrics prepared by means of electrospinning. The foam samples were prepared at RWTH Aachen, which is described in detail in Refs. [10, 11]. The superconducting transition temperature, T_c, of the foam samples is 91.1 K like in the bulk samples. Here it is important to point out that crystallographic orientation was introduced to the foam by using the infiltration growth process on a Y_2BaCuO_5 (211) foam and a seed crystal on top of the structure. This treatment introduced indeed a texture as evidenced by x-ray and neutron diffraction [18].

The Bi-2212 nanowire network fabrics were fabricated by electrospinning as described in Refs. [19–21]. The T_c of the fabric samples is just below 77 K, and previous investigations have shown that the superconducting properties are well developed below 30 K like in the case of bulk Bi-2212 samples [22]. Alternatively, another fabrication technique, the solution blow spinning, was recently developed to produce similar nanowire network fabrics. In this way, YBCO nanowires were produced as well [23].

Magnetic hysteresis loops were recorded out using SQUID magnetometry, for details see, e.g., Ref. [24]. Trapped field (TF) measurement of the foam were carried out using a homemade setup with a scanning Hall probe operating at 77 K. The sample was field cooled in a field of a Nd-Fe-B permanent magnet (0.5 T surface field) in liquid nitrogen. TF profiles were recorded after 15 min waiting time at 1.5-2 mm height above the foam sample surface, which is more rough than that of a bulk sample.

3. Results and discussion

3.1. Nanowire network fabrics

The Bi-2212 nanowire network fabrics consist of long (up to 100 μm) nanowires (diameter $\sim$250 nm) which form a nonwoven fabric material with numerous interconnects between the polycristalline nanowires. These interconnects enable a current flow through the entire sample perimeter. As a result, the nanowire fabrics were found to perform at low temperatures even at large applied magnetic fields up to 10 T as discussed in Refs. [19–21].

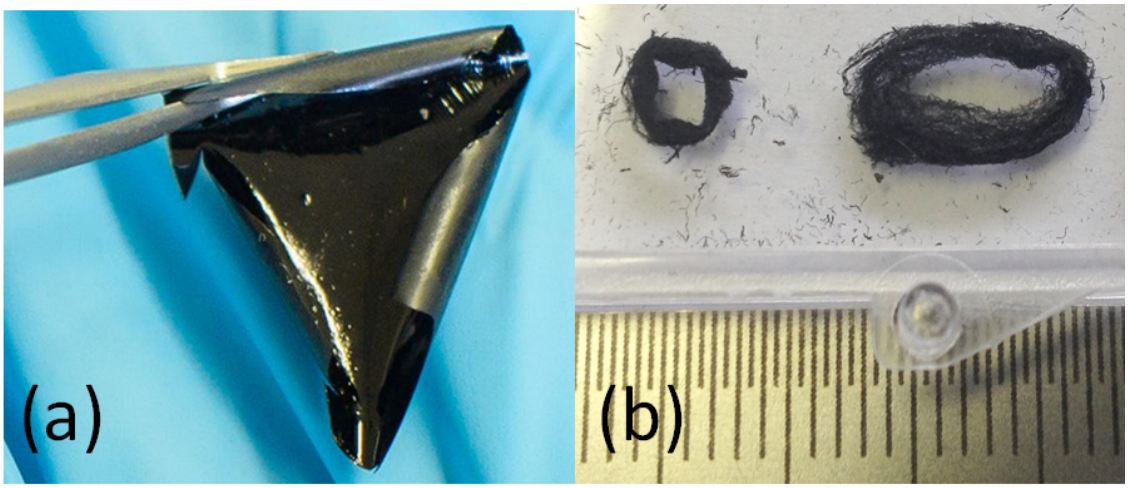

Figure 2. Applications of Bi-2212 nanowire network fabric samples: (a) fully flexible, superconducting foil and (b) completly reacted, donut-shaped nanowire network fabric samples.

Figure 1 (b) already shows that the upscaling of electrospun fabrics is very straightforward. The fully-reacted Bi-2212 nanowire network fabrics are extremely light-weight (only 0.05 g/cm^3 density, porosity 0.9928) [24] and as result, very brittle, which requires additional treatment to make the samples useful for applications. One possible route would be to embed the fully reacted nanowire fabric into a suitable polymer [25], so that a flexible superconducting foil (Fig. 2 (a)) results. Such a flexible foil could easily cover also complicated shapes when being used as a magnetic shield. Another possible application was already discussed in Ref. [26], where the fabric-sample could be used as a large-scale 'superconducting carpet', which would be placed in a thin plastic casing and cooled by streaming liquid nitrogen. In this way, a large platform to levitate magnets above it could be created.

More shaping possibilities are provided in the preform stage which consists of polymer nanowires containing the ceramic precursor material. Here, an easy shaping process is possible: One can cut a small section off and wrap it around a wire to create a donut shape. Figure 2 (b) presents such fully-reacted nanowire donut samples which could be employed as light-weight magnetic shielding.

To bring the nanowire fabric samples towards real applications, it would be a great benefit to have samples with a higher T_c and a less-2D-like behavior as in the case of Bi-2212. A superconducting carpet operating at 77 K with liquid nitrogen as a coolant could be very interesting for automation purposes [26]. The shielding applications could also work at low temperatures/high magnetic field environments, as the resistance measurements on nanowire fabric samples were possible in fields up to 10 T, which one would not expect for such polycrystalline HTSc samples.

3.2. Superconducting foams

The superconducting foams can be applied as trapped field magnets, as the upscaling enables to create foam samples of larger dimensions as bulk samples, avoiding the extremely long oxygenation times required. Furthermore, the foams have much less weight compared to the bulks. The present trapped field values are not spectacular, but here it is important to mention that the current shape of the foams was never optimized for large trapped fields. First experiments [27] had shown trapped fields of ∼400 G, when field-cooling (FC) the a smaller foam sample in a field of 600 mT. In these experiments, it was noted that a broad peak and several sharp peaks resulted.

Figures 3 and 4 show the results of a trapped field experiment on the YBCO foam sample. The sample has dimensions $5 \times 2 \times 2$ cm^3, and was field-cooled in the field of a square Nd-Fe-B magnet (size $30 \times 30 \times 25$ mm^3) which had a surface field of 0.5 T (remanent magnetization 1.3 T). The magnet was located on top of the top surface (with the former seed crystal, labelled (1) – see the inset) of the foam. Figure 3 gives the measured trapped field distributions as 3D surface plots as well as contour plot for the foam sample surface (1) and the side (2), and Fig. 4 shows the measurement results for sides (3) and (4). On all sample sides, we find a trapped field peak, and characteristically, also the presence of several sharp, small peaks. The foam sides (2) and (4), which are 90° off the original field direction, exhibit a broad peak with only a small B_{trap}. Remarkably, there are many of the small sharp peaks on side (4). The measurement on side (3) reveals a negative peak field of −100 G. The measurements clearly demonstrate the presence of two types of currents in the foam sample – one current density, which is running through the entire sample perimeter, resulting in the large, cone-shaped maxima with $B_{\mathrm{trap,max}}$, and one locally distributed current density being responsible for the small sharp peaks. Both currents are percolative, truely 3D currents flowing through the foam struts, and are not confined to planes in the sample. Repeating the scan of B_z reproduces most of these peaks, but the height may vary. We ascribe these peaks to local current loops in the sample, which were formed around local defects (e.g., large pores, pore clusters or non-superconducting struts), and are compressed due to the rearrangement of the internal field, B_i, when removing the external field. Similar observations were made already in Ref. [27], where only the surface (1) close to the seed crystal was measured. Here we have to note that the Hall probes measure only the z-component of B, which implies that current paths along the z-axis without a z-component of the generated magnetic field will not be detected. Only the *(a,b)*-projection of the real circulating 3D currents will be measured, and, the various contributions to it are weighted relative to their distance to the scanning Hall probe.

The measured trapped field values are still smaller than those of YBCO bulks, but regarding the difference in current density and the reduced weight of the foam samples, the results are not so bad. Also, most IG-processed bulks were found to exhibit still smaller trapped fields

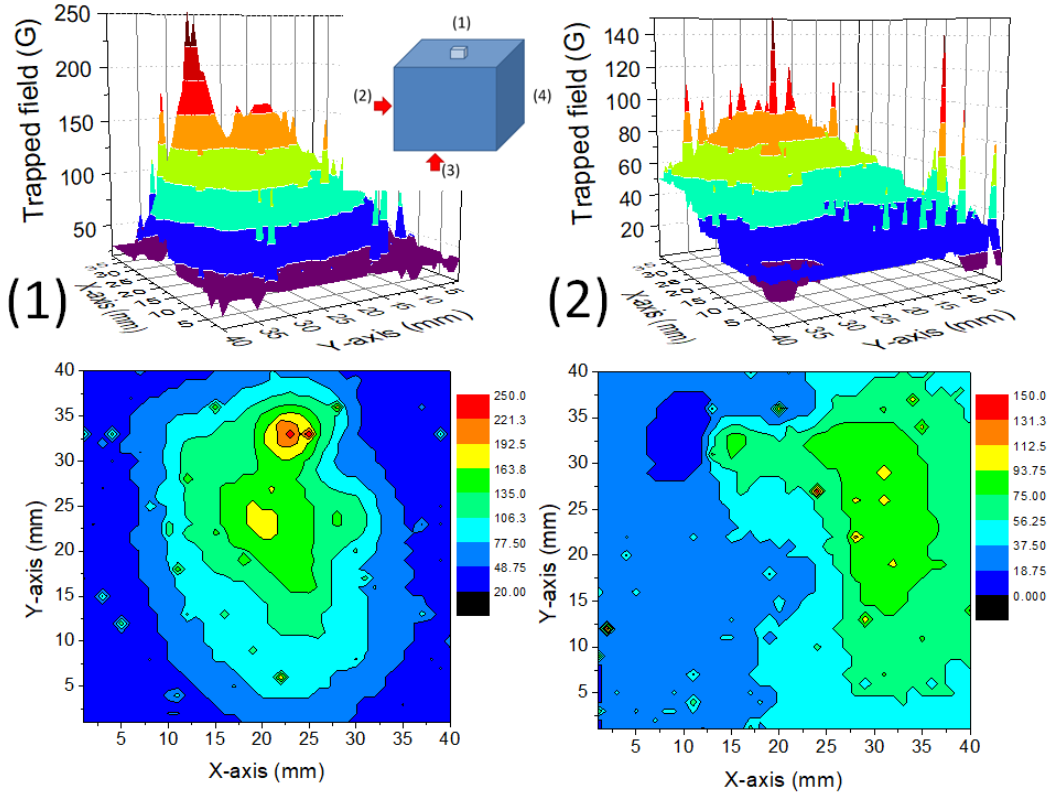

Figure 3. Trapped field measurements on a foam sample. Distribution of B_z measured by scanning Hall probe on sides (1) and (2) of the foam sample. The inset gives a schematic drawing of the foam sample and the nomenclature. The permanent magnet in the FC cooling process was placed on side (1).

as the MTMG-processed bulks. Furthermore, the present foam sample is 14 years old and has underwent many experiments as shown in Fig. 5 below. Here, it is important to point out that the present sample shape was never optimized for trapped field measurements, nor the texture of the sample, which has a dominating orientation, but even magnetization measurements on single struts still reveal signs of granularity [28]. A simple estimation of the overall transport current density in the foam sample can be done using the size of the trapped field peak (B_{trap}) with the relation [29]

$$J_c R \propto B_{\mathrm{trap}}/\mu_0 \quad . \tag{1}$$

With the maximal trapped field of 250 G and $R = 15$ mm, we obtain $J_c = 130$ A/cm^2.

Due to the multi-peak trapped field distribution as seen in Figs. 3 and 4, this estimation gives the lower boundary for the real critical current density flowing in the sample. This observation points out that the current flow in such porous samples is more complex as in bulk samples, so we need a closer look to it.

Concerning the current flow in porous high-T_c materials, we have to be aware that these are polycrystalline materials, so we have to consider two different contributions; the intergranular ($J_{\mathrm{c,inter}}$) and intragranular ($J_{\mathrm{c,intra}}$) currents. The intragranular currents are controlled by the flux pinning and are as high as those of single crystals or bulk samples, whereas the intergranular currents are affected by the grain boundaries between the superconducting grains and by the

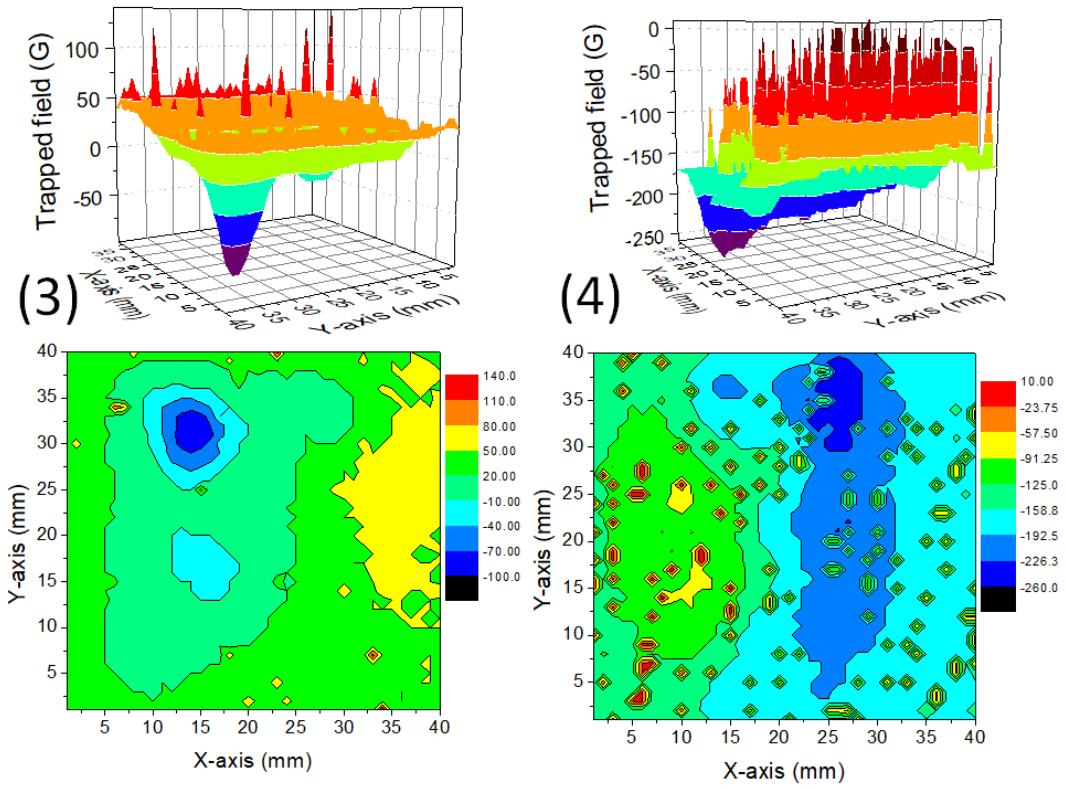

Figure 4. Distribution of B_z measured by scanning Hall probe sides (3) and (4).

relative orientations of the anisotropic granules to each other. This describes the case of dense, bulk polycrystalline samples. In porous samples, there is an additional contribution due to the percolative current flow caused by the porosity and the spacial orientation of the foam struts to the external field. In case of the nanowire networks, the contacts formed by the interconnects between the nanowires provide another limiting factor. Therefore, the overall currents flowing through the entire sample are limited by all these factors, which is the main drawback for the porous superconducting materials.

Figure 5 presents $J_{\mathrm{c,intra}}$ for the Bi-2212 nanowire fabrics. The data for $J_{\mathrm{c,intra}}$ (open symbols) stem from measured magnetization loops of extended pieces of the nanowire fabric, and were evaluated using the Bean model and corrected for porosity by a factor 1/0.0072. Details of this calculation using the extended critical state model (ECSM) on the measured magnetization data can be found in Ref. [24]. The Bi-2212 nanowires show relatvely high current densities only at temperatures below 30 K, which is in stark contrast to the YBCO foam, which is also shown in Fig. 5 using full symbols for the intragranular current density measured on a single foam strut at $T = 60$ K and 77 K [28]. Therefore, liquid nitrogen can be used as coolant for the YBCO foam samples. The lower limit of the overall current density determined from the trapped field data is given also in Fig. 5 for comparison. Calculating this overall current density for the nanowire fabric sample yields about 0.05 A/cm^2.

The YBCO foam shows much higher values of H_{irr} than the Bi-2212 nanowire fabric sample, being comparable to those of IG-processed bulk samples. The H_{irr} reaches 7 T already at 77 K, which renders the measurement difficult [28]. The irreversibility field is known to be strongly

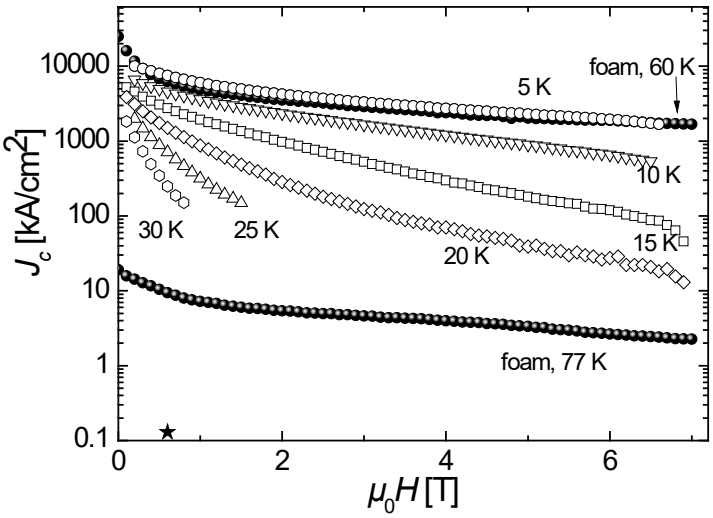

Figure 5. Critical current densities of the YBCO foam and the Bi-2212 nanowire network fabrics. The open symbols give the intragranular current density $J_{\mathrm{c,intra}}$ of the Bi-2212 nanowires; the full symbols give the intragranular current density $J_{\mathrm{c,intra}}$ measured on an individual YBCO foam strut piece at 60 K and 77 K for comparison. The star indicates the overall current density of the foam sample determined from the trapped field plots at 77 K.

dependent on the pinning strength and on the scale of the current circulation [30, 31]. As also texture is achieved in the YBCO foam samples [18], this is very promising for future improvement of the overall critical current densites of such foam samples.

The superconducting YBCO foams could see many different applications which make use of the efficient cooling process, e.g., for fault current limiters, which was already discussed in the first publications on foams [10, 11]. Cooling of superconducting foam structures from room temperature to 77 K proceeds about ten times faster compared to respective bulk materials of the same mass and composition [6]. This can directly be demonstrated when cooling a foam sample in liquid nitrogen, e.g., to test the levitation properties on a magnetic rail consisting of 3 Nd-Fe-B magnets in a row (S-N-S configuration, [32]) as shown in Fig. 6. When operating on such a magnetic rail, the foam sample is cooled so well that it takes ∼5 min to warm up again. Furthermore, the lift height of the foam sample is much higher than that of an YBCO bulk sample due to the reduced weight. Another interesting possibility would be to turn around the situation of the levitation experiment: Using long pieces of foam would create an easily coolable superconducting rail, where magnetic objects can levitate upon. Such a superconducting rail system could be cooled very effectively by liquid nitrogen being pumped through.

The examples presented are not yet all possibilities for superconducting foam samples. Superconducting foams with small open porosity can easily be continuously reinforced, e.g. with resins, to improve their mechanical properties and, thus, to overcome the forces encountered in levitation and quasi-permanent magnet applications [33]. Also an electroplating process to further improve the mechanical strength as done for metallic Al foams [9] could be carried out here, as well as impregnation using resins. This will contribute to avoid the cracking problems of bulk superconductor samples prevailing when trapping large magnetic fields at lower temperatures. The large amount of possible applications of foam samples suggest that further development of this sample type is an important task for the future. Combining the

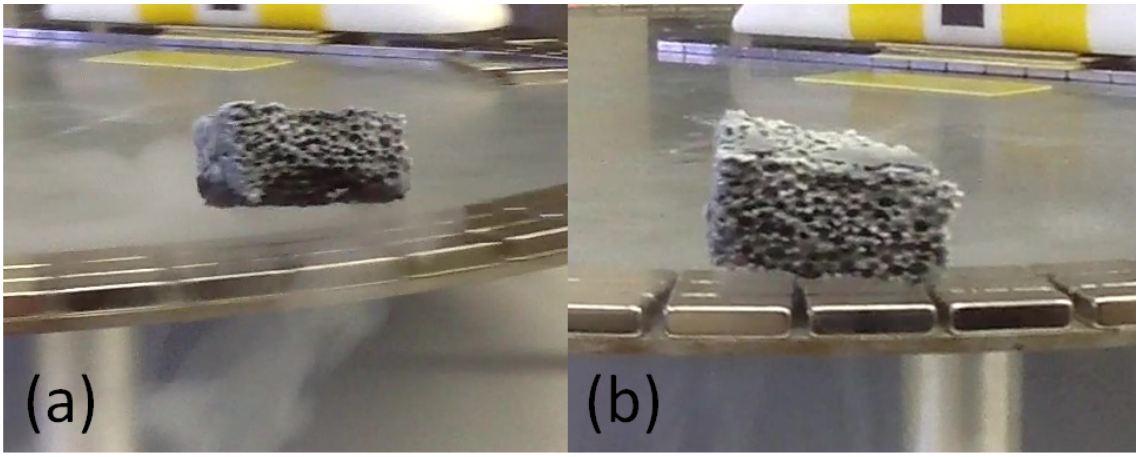

Figure 6. Superconducting foam levitating above a magnetic rail. (a) shows the foam sample at full speed running on the rail, and (b) gives the foam sample when being close to warm up.

latest developments concerning the IG processing of HTSc materials, the optimization of the sample shape for the given task and improved understanding of the open porous structure can lead to unique types of superconducting samples to fulfill different demands of applications. This will be the goal for future experimental work concerning a second generation of superconducting foam samples.

4. Conclusions

To conclude, porous high-T_c superconducting cuprates are very promising materials for applications wherever the sample weight or the cooling efficiency counts. This is given, e.g., in space experiments, for fault current limiters, and trapped field applications in rotating machinery. The achieved trapped field values are still small, but promising and the cooling efficiency can be demonstrated in simple levitation experiments. The future work will require also a deeper understanding of the current flow in such samples, combining already existing modelling approaches of mechanical properties of metallic foams with modelling of the superconducting current flow.

Acknowledgments

We thank X. L. Zeng, T. Karwoth for the work on electrospinning, G. Schmitz (ACCESS, RWTH Aachen, Germany) for the foam sample and K. Berger, B. Douine and Q. Nouailhetas (GREEN, Nancy, France) for valuable discussions concerning the foam materials. This work is supported by DFG-ANR grant Ko 2323/10 ("Superfoam"), SIT start-up grant and Volkswagen foundation, which is gratefully acknowledged.

References

[1] Larbalestier D C, Gurevich A, Feldmann D M and Polyanskii A 2001 *Nature* **414** 368
[2] Gurevich A 2011 *Nature Mater* **10** 255
[3] Noudem J G 2011 *J Supercond* **24** 105
[4] Johansen T H 2000 *Supercond Sci Technol* **13** R121
[5] Diko P 2004 *Supercond Sci Technol* **17** R45
[6] Nettleship I 1996 *Key Eng. Mater.* **122** 305
[7] Colombo P 2002 *Key Eng Mater* **206-213** 1913
[8] Hill Ch and Eastoe J 2017 *Adv Colloid Interface Sci* **247** 496

[9] Jung A, Diebels S, Koblischka-Veneva A, et al. (2013) *Adv Eng Mater* **16** 15
[10] Reddy E S and Schmitz G J 2002 *Am Ceram Soc Bull* **81** 35
[11] Reddy E S, Herweg M and Schmitz G J 2003 *Supercond Sci Technol* **16** 608
[12] Petrov M I, Tetyueva T N, Kveglis L I, Efremov A A, Zeer G M, Shaikhutdinov, K A, Balaev D A, Popkov S I and Ovchinnikov S G 2003 *Tech Phys Lett* **29** 986
[13] Fiertek P and Sadowski W 2006 *Material Science Poland* **24** 1103
[14] Fiertek P, Andrzejewski B and Sadowski W 2010 *Rev Adv Mater Sci* **23** 52
[15] Terent'ev K Yu, Gokhfeld D M, Popkov S I, Shaikhutdinov K A and Petrov M I (2011) *Phys Solid State* **53** 2409
[16] Eisterer M, Moon S H and Freyhardt H C 2016 *Supercond Sci Technol* **29** 060301
[17] Durrell J H, Ainslie M D, Zhou D, Vanderbemden P, Bradshaw T, Speller S, Filipenko M and Cardwell D A 2018 *Supercond Sci Technol* **31** 103501
[18] Noudem J G, Guilmeau E, Chateigner D, Lambert S, Reddy E S, Ouladdiaf B and Schmitz G J 2004 *Physica C* **408410** 655
[19] Zeng X L, Koblischka M R and Hartmann U 2015 *Mat Res Express* **2** 095022.
[20] Koblischka M R, Zeng X L, Karwoth T, Hauet T and Hartmann U 2016 *IEEE Trans Appl Supercond* **26** 1800605
[21] Koblischka M R, Zeng X L, Karwoth T, Hauet T and Hartmann U 2016 *AIP Adv* **6** 035115
[22] Koblischka M R and Sosnowski J 2005 *Eur J Phys B* **44** 277
[23] Rotta M, Zadorosny L, Carvalho C L, Malmonge J A, Malmonge L F and Zadorosny R 2016 *Ceram Int* **42** 16230
[24] Zeng X L, Karwoth T, Koblischka M R, Hartmann U, Gokhfeld D, Chang C and Hauet T 2017 *Phys Rev Mater* **1** 044802
[25] Haupt S G, Riley G R, and McDevitt J T (1993) *Adv Mater* **5** 755
[26] Koblischka M R and Koblischka-Veneva A 2018 *AIMS Material Sci* **5** 1199
[27] Bartolomé E, Granados X, Puig T, Obradors X, Reddy E S and Schmitz G J 2004 *Phys Rev* B **70** 144514
[28] Koblischka M R, Koblischka-Veneva A, Chang C, Hauet T, Reddy E S and Schmitz G J 2018 *IEEE Trans. Appl. Supercond.* DOI: 10.1109/TASC.2018.2880334.
[29] Bean C P 1962 *Phys Rev Lett* **8** 250
[30] Ihara N and Matsushita T 1996 *Physica* C **257** 223
[31] Matsushita T, Otabe E S, Wada H, Takahama Y and Yamauchi H 2003 *Physica* C **397** 38
[32] Santosh M and Koblischka M R 2014 *Eur J Phys Educ* **5**(4) 1
[33] Tomita M and Murakami M 2003 *Nature* **421** 517